Simulation of knock probability in an internal combustion engine

Huanyu Di and Tielong Shen*
Department of Engineering and Applied Sciences, Sophia University, Kioicho 7-1, Chiyoda-ku, Tokyo 102-8554, Japan

(Received 11 February 2018; revised manuscript received 21 May 2018; published 3 July 2018)

In spark-ignition internal combustion engines, fluctuations of the in-cylinder pressure trace and the tendency of combustion knock are usually different from one cycle to another. These cycle-to-cycle variations are affected by the initial state at ignition time and the subsequent burning. The occurrence of the phenomena is unpredictable, and their stochastic nature offers challenges in the optimization of engine control strategies. In this paper, a simulator providing a series of cycle-to-cycle varied in-cylinder pressures is introduced. The Wiebe function and Livengood-Wu integration are used to describe the determinacy of combustion. Various means, including the Markov chain, are introduced to express the stochastic quantities during combustion. In addition, the combustion of a given knock probability is simulated.

DOI: 10.1103/PhysRevE.98.012102

I. INTRODUCTION

It is well known that combustion in a chamber is a phenomenon with stochasticity[1–3]. In a spark-ignited internal engine, the combustion event in the cylinder performs cycle-by-cycle under external actuation such as fuel injection, valve timing, ignition, etc. However, the stochasticity in combustion can be observed even under conditions without external actuation and changing thermal environments. As a result, this randomness leads to the cycle-to-cycle variation of engine output such as indicated mean efficient pressure (IMEP), thermal efficiency, and emissions. In the past three decades, much literature on cycle-to-cycle combustion has been published [4–10]. For example, a statistical analysis of the cyclic combustion event is explained from the view of physics [11], and experimental analyses on cyclic variation have also been provided [12]. In addition, attempts at modeling the cyclic transient in the cylinder state have been proposed in Ref. [13], which focuses on the cyclic variation influence of the residual gas fraction.

Meanwhile, motivated by the strict regulation on emission and energy consumption for production engines, the attention of developing technology has been recently focused on high-efficiency combustion engines in the automotive industry [14]. Furthermore, as an efficient approach, model-based development has been a new research trend in the automotive industry [15]. From the view of control algorithm development for the electrical control unit (ECU) of engines, 1D models that represent the in-cylinder behavior of combustion engines are most widely used in control design and simulation. However, mathematical representation of the cycle-to-cycle variations of in-cylinder combustion, especially the stochastic characteristics of in-cylinder combustion phenomena, still remain to be studied.

In this paper, a simple 1D dynamic model is introduced to simulate combustion with cycle-to-cycle variations. The in-cylinder pressure and knock are chosen to be simulated. The in-cylinder pressure can illustrate the combustion progress, and the random knock is directly caused by the cycle-to-cycle variation. The Markov chain and multivariate normal distribution are introduced to represent the randomness and chaos of combustion, respectively, according to the physical reality. The proposed 1D model can simulate the statistical information of numerous cycles successfully, conditional on ignoring the chaotic and stochastic characteristics of real fluids and combustion. Table I describes the variables used in this paper.

II. PHYSICAL BACKGROUND AND PROBLEM DESCRIPTION

According to the fact that commonly used engines of gasoline-fueled automobiles have four strokes and operate under an Otto cycle, these engines are also applied in this study.

The working process of the experimental engine is shown in Fig. 1. In a spark-ignition engine, the downward moving piston enlarges the volume of the cylinder, and fresh air and fuel are inducted through the intake valve during the first intake stroke. Then, the mixture of air and fuel are compressed by the upward moving piston in the compression stroke. Just before reaching the minimal cylinder volume, the combustion is initiated by a high-voltage spark, and the power stroke follows. The explosion of hot gases pushes the piston downward [16]. The most important phenomenon focused on in the simulator of the spark ignition engine is the in-cylinder combustion. The energy is provided by combustion, and the randomness and chaos of the engine are caused by the combustion; thus, they are the focus in this work. As the piston moves upward again in the exhaust stroke, the discharged gases are vented through the exhaust valve. The intake, compression, combustion, and exhaust stroke compose one engine cycle. The engine is operated cycle by cycle.

To illustrate the piston position and working progress of the engine, crank angle θ is used in this simulator. The crank shaft is an important link of the chain transferring power from the

*tetu-sin@sophia.ac.jp

TABLE I. Nomenclature.

Variable	Description
θ	Crank angle (deg)
p	In-cylinder pressure (pa)
V	In-cylinder volume (m^3)
T	In-cylinder temperature (K)
Q	Heat release from start of combustion (J)
R	Ideal gas constant($8.314 J\,mol^{-1} \cdot K^{-1}$)
κ	Specific heat ratio of the mixed gas
θ_{10}	Crank angle interval from start of combustion until 10% of the mass burnt (deg)
θ_{90}	Crank angle interval from start of combustion until 90% of the mass burnt (deg)
Q_{total}	Total heat release of the indicated cycle (J)
$\boldsymbol{\Theta}$	Parameter of the Markov chain
$\mathcal{N}$	Normal distribution
x_b	Mass fraction burnt
I	Livengood-Wu knock integration
O_N	Octane number of fuel
K	Expected knock probability (%)
K^*	Knock probability (%)

piston to the load in the engine. The crank angle ranges from 0 to 720 degrees in each cycle. The crank angle equals 0 when the intake stroke starts, and the in-cylinder volume is minimal.

When the in-cylinder pressures are expressed against the crank angle, the disparity of the pressure trace can easily be observed from one cycle to another. As shown in Fig. 2, the region where the pressure traces diverge coincides with the combustion period. Those cycle-to-cycle variations are affected by the early flame development and subsequent flame front propagation [16]. To describe the cycle-to-cycle variations, the in-cylinder combustion needs to be studied in detail.

Violent cycle-to-cycle variations can lead to an abnormal phenomenon called knock. Knock is a form of abnormal combustion in spark-ignition engines, which is characterized by high pressure oscillations [17]. After spark ignition, the flame front, which is the surface separating the burned and unburned gases, moves from the ignition plug to the entire cylinder. Part of the unburned gas is compressed by the piston and the burned gas. The high pressure and temperature in

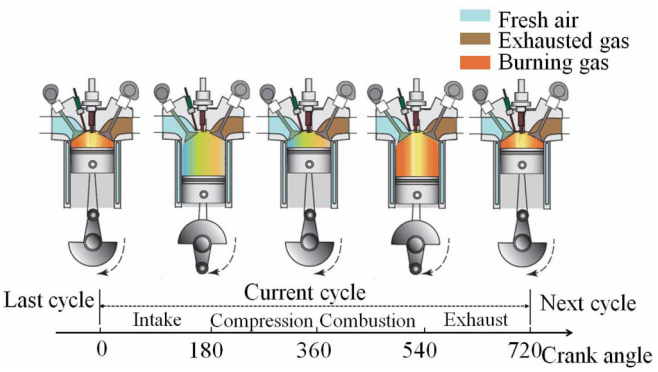

FIG. 1. Schematic view of spark-ignition engine.

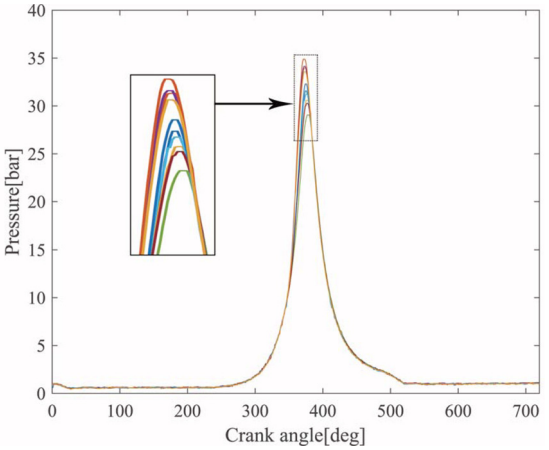

FIG. 2. In-cylinder pressure of 10 successive cycles.

this area cause spontaneous combustion to occur. The knock vibration is caused by this double ignition, which reduces the engine efficiency. Heavy knock may lead to engine failure, so when studying cycle-to-cycle variations, a method to monitor the knock is needed.

III. EXPERIMENT AND DATA PROCESSING

To obtain the physics of cycle-to-cycle combustion, an experiment is conducted on a test bench, in which a Toyota 2ZR-FXE gasoline engine is coupled to a Horiba Dynas3-LI250 low inertial alternative current dynamometer as shown in Fig. 3. The engine parameters are presented in Table II. The control and measurement system of the test bench includes an electronic engine control unit, a SPARC controller of the dynamometer, and a dSPACE1006 multiprocessor system connected to a personal computer. In addition, a high-speed data acquisition card, dSPACE2004, is equipped to collect the submillisecond pressure data.

In the experiment, the engine is operated under fixed operating conditions, which include intake valve closing (IVC) at 250 degrees and ignition angle at 344 degrees. In addition,

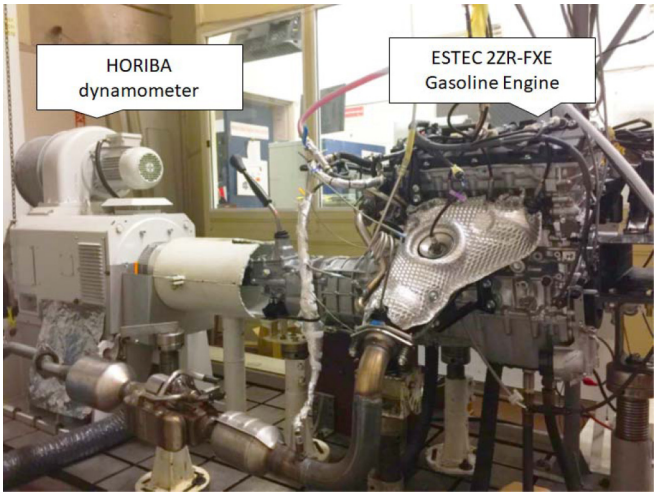

FIG. 3. Configuration of the engine-dynamometer test bench.

TABLE II. Specification of the experimental gasoline engine.

Engine type	2ZR-FXE, L-type
Displacement	1797 ml
Cylinder number	4
Compression ratio	13.0
Maximal speed	6000 rpm
Maximal power	72 kW @ 5200 rpm
Maximal torque	142 Nm @ 3600 rpm
Cylinder diameter	80.5 mm
Stroke	88.3 mm

engine speed is restricted at 1200 rpm (revolution per min) by the dynamometer. Under this condition, the combustion knock probability is 3%, which is important information to adjust the parameters in the knock model. During the experiment, the in-cylinder pressure is measured against the crank angle. As shown in Fig. 4, the experimental data are the pressure-crank angle curve of 1979 cycles.

The experimental data are processed cycle by cycle to derive the randomness of combustion. A set of parameters are selected to characterize the combustion process. According to the structure of the combustion model, which is introduced in the next section, the set of parameters are selected as Q_{total}, θ_{90}, and θ_{10}. Q_{total} is the total heat release of the current cycle. θ_{90} is the crank angle interval from the start of combustion until 90% of the mass burnt, which indicates the end of combustion. θ_{10} is the crank angle interval from the start of combustion until 10% of the mass burnt. Parameter θ_{10} is the symbol of ignition delay, which means the delay of the crank angle from ignition to the beginning of combustion.

When the measured data of each cycle are studied, there are two widely accepted assumptions. First is that the mixed gas in the cylinder is treated as an ideal gas, from which the following can be inferred:

$$pV = nRT, \tag{1}$$

$$U = \tfrac{1}{1-\kappa} nRT, \tag{2}$$

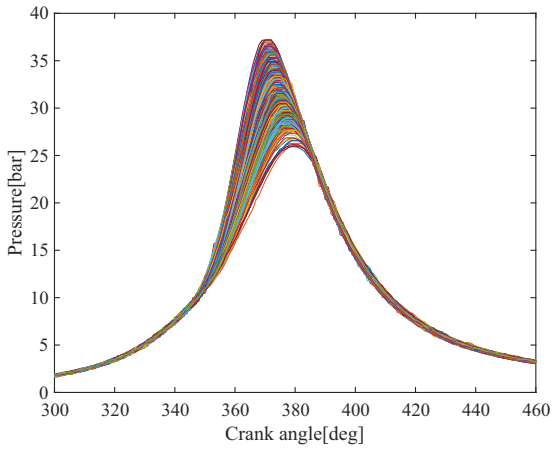

FIG. 4. Measured in-cylinder pressure.

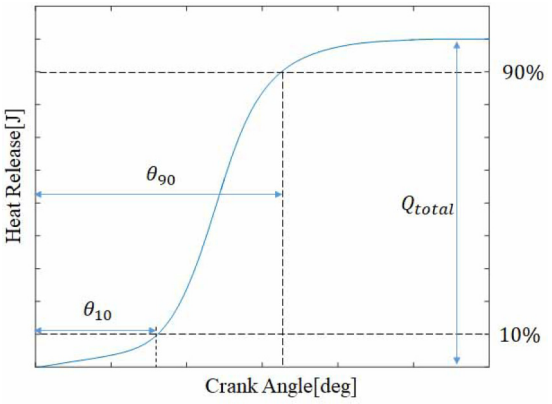

FIG. 5. The schematic diagram of the calculation of Q_{total}, θ_{90}, and θ_{10}.

where n is the mole number of the mixed gas in the cylinder, and U is the internal energy of the gas.

The second assumption is that the in-cylinder combustion is an isolated process. The heat loss is ignored:

$$dQ = -dU + pdV. \tag{3}$$

Under the constraints of Eqs. (1) and (2), Eq. (3) can be rewritten as

$$\begin{aligned} dQ &= \frac{1}{\kappa - 1} nRdT + pdV \\ &= \frac{1}{\kappa - 1} d(pV) + pdV \\ &= \frac{\kappa}{\kappa - 1} pdV + \frac{1}{\kappa - 1} Vdp. \end{aligned} \tag{4}$$

The in-cylinder combustion is started by the spark when the crank angle reaches the spark angle ($SA = 334$ degrees in this paper). Thus, the heat release at each crank angle can be calculated as

$$Q = \begin{cases} 0 & 0 < \theta \leqslant 334 \\ \displaystyle\int_{334}^{\theta} \left(\frac{dQ}{d\theta} \right) d\theta & 334 < \theta \leqslant 720 \end{cases}. \tag{5}$$

For every cycle, the heat release (Q) curve can be plotted against the crank angle (θ). The measured parameters Q_{total}, θ_{90}, and θ_{10} can be calculated according to the heat release curve of each cycle, as shown in Fig. 5.

IV. PROPOSED MODEL FOR SIMULATION

The purpose of proposing this model is to simulate the detail states (such as pressure) of the engine working at a certain knock probability. The model needs to calculate quickly enough to be used for model-based control. Thus, the 1D model is introduced to make sure the calculations are simple, and various improvements are added to simulate the cycle-to-cycle variations.

The 1D model ignores the special distribution and hydromechanic performance, which lead to the cycle-to-cycle variations. To simulate the stochastic cycle-to-cycle variations, random parameters need to be introduced to represent those phenomena. In addition, based on the observation of the

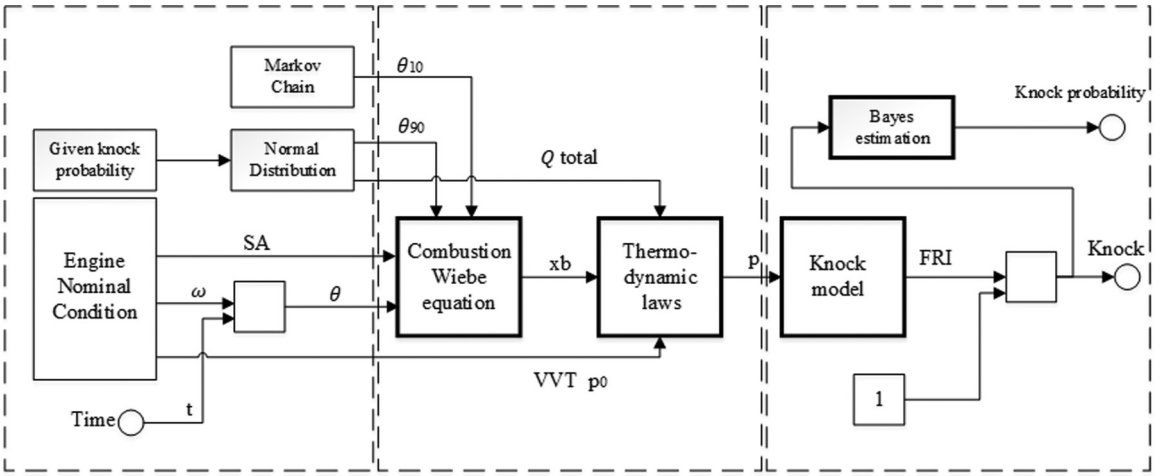

FIG. 6. Structure of the simulation model.

experiments, the knocking probability under the same engine working conditions is not constant because of the uncontrolled environment condition. In the presented simulation, the parameters of the combustion model need to match the variable knock probability.

Therefore, the model is represented by three parts. The first part is to generate the random parameter and describe the nominal condition of the engine. The second part is to simulate the in-cylinder combustion and revolute the in-cylinder pressure. The last part is to diagnose if knock occurs and calculate the knock probability. The simulator structure is shown in Fig. 6.

A. Generation of combustion randomness

To simulate the cycle-to-cycle varied combustion, the parameters Q_{total}, θ_{90}, and θ_{10} are dealt with as a random number. If the distribution of parameters are designed appropriately, they influence the accuracy of the proposed model. According to the measured data and the physical background, the distribution of Q_{total} and θ_{90} is selected as the multivariate normal distribution, and a Markov chain is chosen to describe the evolution of θ_{10}.

1. Multivariate normal distribution

The parameters Q_{total}, θ_{90}, and θ_{10} of each cycle are ascertained by the data processing presented in Sec. III. The experimental distribution of the three parameters of all 1979 cycles can be acquired. As shown in Fig. 7, the experimental mean μ_θ and variance σ_θ^2 of θ_{90} are

$$\mu_\theta = 43.0424, \quad \sigma_\theta^2 = 4.6115. \tag{6}$$

In the proposed model, the θ_{90} is chosen to be the parameter to characterize the cycle-to-cycle variations. When the nominal operating condition is fixed, the cycle-to-cycle variations influences knock probability significantly. To get a given knock probability, the distribution of θ_{90} must be adjusted. When the knock probability is 3%, which is same as the experiment, a normal distribution characterized by the average value of 43.0424 and the variance of 4.6115 can be selected to describe the distribution of parameters θ_{90}. The θ_{90} of the current cycle can be obtained randomly based on the normal distribution:

$$\begin{aligned} p(\theta_{90}) &= \mathcal{N}\left(\theta_{90}|\mu_\theta,\sigma_\theta^2\right) \\ &= \frac{1}{\left(2\pi\sigma_\theta^2\right)^{1/2}} e^{-\frac{1}{2\sigma_\theta^2}(\theta_{90}-\mu_\theta)^2}. \end{aligned} \tag{7}$$

The parameter Q_{total} can also be described as a normal distribution. However, Q_{total} are not independent from the parameter θ_{90} according to the experimental data, as shown in Fig. 8. The correlation of θ_{90} and Q_{total} can be quantified by Pearson product-moment correlation coefficient $r_{\theta Q}$, which equals 0.5608. There is a larger θ_{90} in the cycle when the heat release Q_{total} is higher. Due to this independence, the distribution of Q_{total} needs to be calculated by the covariance matrix $\mathbf{\Sigma}$ and the θ_{90} of the current cycle. Then, the covariance matrix of θ_{90} and Q_{total} is expressed as

$$\mathbf{\Sigma} = \begin{bmatrix} \sigma_\theta^2 & \sigma_\theta\sigma_Q r_{\theta Q} \\ \sigma_\theta\sigma_Q r_{\theta Q} & \sigma_Q^2 \end{bmatrix}, \tag{8}$$

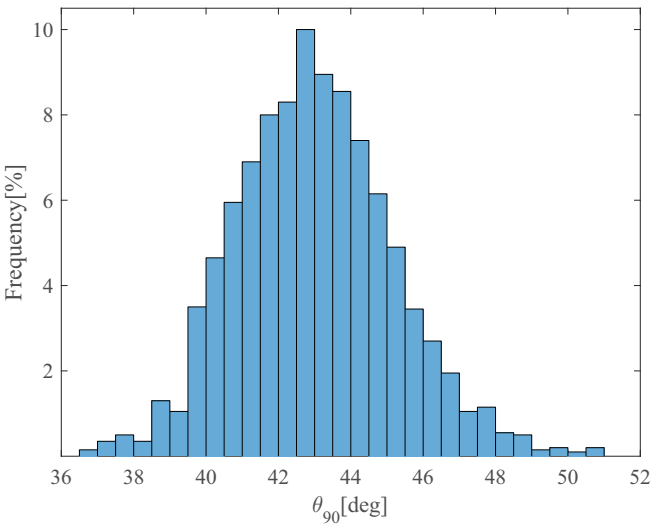

FIG. 7. Experimental θ_{90} frequency distribution.

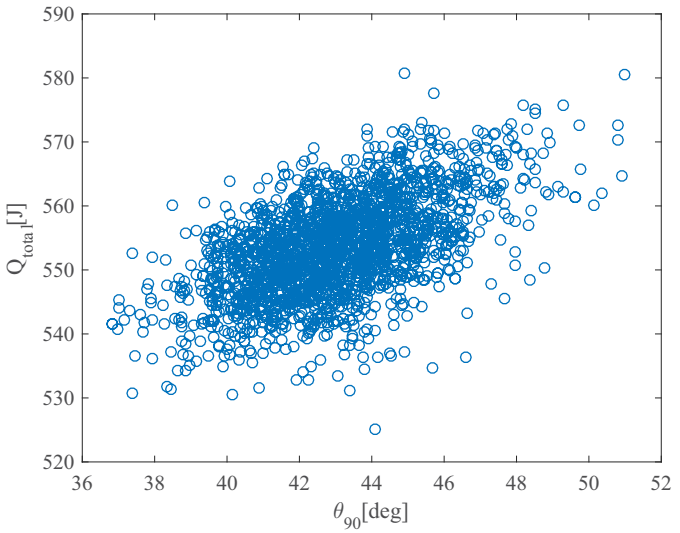

FIG. 8. Relationship of the total heat release Q_{total} (y axis) and θ_{90} (x axis) according to the experimental data.

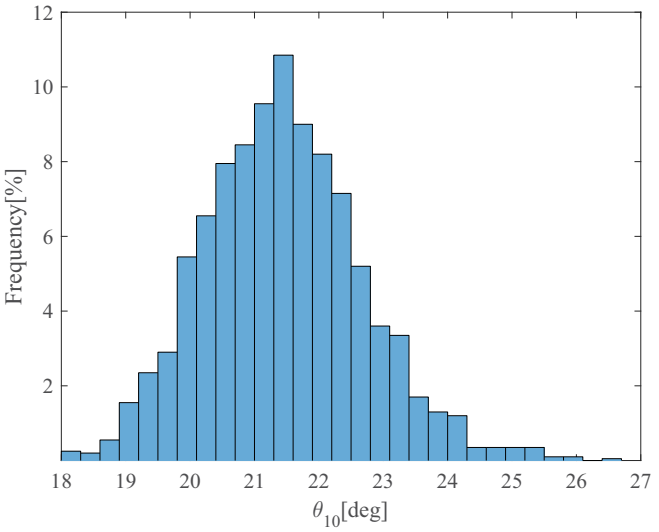

FIG. 9. Experimental θ_{10} frequency distribution.

where

$$r_{\theta Q} = 0.5608, \quad \sigma_Q^2 = 60.0462$$

σ_Q^2 is the variance of Q_{total}. The σ_Q^2 is given as 60.0462 according to the experimental data. When θ_{90} is decided, the distribution of Q_{total} can be calculated by the covariance matrix based on the calculation of conditional probability[18]. The parameter Q_{total} of the current cycle can be obtained randomly based on the multivariate normal distribution:

$$p(Q_{\text{total}}|\theta_{90}) = \mathcal{N}\left(\mu_{Q|\theta}, \Lambda_{QQ}^{-1}\right), \tag{9}$$

where

$$\mathbf{\Lambda} = \begin{bmatrix} \Lambda_{\theta\theta} & \Lambda_{\theta Q} \\ \Lambda_{Q\theta} & \Lambda_{QQ} \end{bmatrix} = \mathbf{\Sigma}^{-1},$$

$$\mu_{Q|\theta} = \mu_Q - \Lambda_{QQ}^{-1}\Lambda_{Q\theta}(\theta_{90} - \mu_\theta),$$

2. Markov chain

As shown in Fig. 9, there is a slight asymmetry of the experimental θ_{10} distribution. The mean value $\mu(\theta_{10})$ and variance $\sigma^2(\theta_{10})$ can be calculated, but the normal distribution is not suitable to describe it:

$$\mu(\theta_{10}) = 21.4494, \ \sigma^2(\theta_{10}) = 1.5260. \tag{10}$$

For in-cylinder combustion, θ_{10} can represent the ignition delay that is an important index of combustion and influence the in-cylinder pressure in the current cycle. The ignition strongly depends on how difficult it is for the in-cylinder gas to be set on fire. Additionally, the fraction and temperature of residual gas of prior cycle influence the difficulty of ignition. Because of this physical background, the distribution of θ_{10} is not suitable to be treated as a normal distribution. As mentioned, the combustion states of prior cycle have some influence on the θ_{10} of next one cycle. The distribution of θ_{10} can represent the combustion states to some extent. In this case, if the distribution of θ_{10} is regarded as a state, the process of continuous in-cylinder combustion has a Markov property, which means the probability of whether the distribution of θ_{10} will change only depends on the current distribution of θ_{10}. To describe the process in which the probability of one state changes to another only depends on the current state, a Markov chain is used extensively. Thus, θ_{10} can be generated by a discrete-time Markov chain.

As mentioned above, to get the stochastic θ_{10}, a two-hidden-states Markov chain is modeled. There are two states, each of which represents one certain normal distribution of stochastic θ_{10}. It is called a hidden state because it cannot be confirmed by the measured data. The value of θ_{10} is obtained at discrete time t for one state and at time $t+1$ the state that may change into another at a certain probability.

The Markov chain can be described by $\mathbf{\Theta}$:

$$\begin{aligned} \mathbf{\Theta} &= (\boldsymbol{A}, \boldsymbol{B}, \boldsymbol{\pi}), \\ \boldsymbol{A} &= \begin{bmatrix} a_{11} & a_{12} \\ a_{21} & a_{22} \end{bmatrix}, \ \boldsymbol{B} = \begin{bmatrix} \mathcal{N}_1 \\ \mathcal{N}_2 \end{bmatrix}, \ \boldsymbol{\pi} = [\pi_1, \pi_2]. \end{aligned} \tag{11}$$

The figure a_{ij}, which is the element of stochastic transition matrix $\boldsymbol{A}$, describes the probability that if θ_{10} is given by state i at time t, then at time $t+1$, θ_{10} is calculated by state j. The distribution $\mathcal{N}_i(\theta_{10}|\mu_i, \sigma_i^2)$ is the element of vector $\boldsymbol{B}$ that defines the probability distribution of θ_{10} at the certain state i. The element of the initial state distribution vector $\boldsymbol{\pi}$ is the number π_i that defines the probability of the initial state of i.

To find the unknown parameters of a Markov chain, the Baum-Welch Algorithm is widely used [18]. We express the sequence of the observed data as O and the sequence of hidden state as I, where L is the length of the measured data:

$$\begin{aligned} \boldsymbol{O} &= (o_1, o_2, \cdots, o_L), \\ \boldsymbol{I} &= (i_1, i_2, \cdots, i_L). \end{aligned} \tag{12}$$

The evaluation criteria of the Markov chain parameter $\mathbf{\Theta}$ can be presented as the log-likelihood function $F(\mathbf{\Theta})$ of the experimental data generated by a certain Markov chain. The log function is monotonically increasing, and when the

log-likelihood function reaches its upper bound, the likelihood function is maximum, which means that the parameter Θ is selected as most likely right:

$$F(\boldsymbol{\Theta}) = P(\boldsymbol{O}|\boldsymbol{\Theta})\log P(\boldsymbol{O}|\boldsymbol{\Theta}). \tag{13}$$

To find the best coordinated parameter $\boldsymbol{\Theta} = (\boldsymbol{A},\boldsymbol{B},\boldsymbol{\pi})$, the Baum-Welch algorithm is used to find a group of parameters to make the function $F(\boldsymbol{\Theta})$ reach its upper bound. The Baum-Welch algorithm is also used to find a new function Q that is smaller than F, and then, the parameter $\boldsymbol{\Theta}$ is changed step-by-step to enlarge function Q and find this upper bound. Function Q is defined as

$$Q(\boldsymbol{\Theta},\hat{\boldsymbol{\Theta}}) = \sum_{\boldsymbol{I}} P(\boldsymbol{O},\boldsymbol{I}|\hat{\boldsymbol{\Theta}})\log P(\boldsymbol{O},\boldsymbol{I}|\boldsymbol{\Theta}). \tag{14}$$

Function Q is used in iterative optimization. $\boldsymbol{\Theta}$ is the unknown parameter needed to be found to enlarge Q, and $\hat{\boldsymbol{\Theta}}$ is the known parameter that is found in the last step. Thus, it can be proven that

$$\begin{aligned} F(\boldsymbol{\Theta}) =& P(\boldsymbol{O}|\boldsymbol{\Theta})\log P(\boldsymbol{O}|\boldsymbol{\Theta}) \\ =& P(\boldsymbol{O}|\boldsymbol{\Theta})\log \sum_{\boldsymbol{I}} P(\boldsymbol{I})\frac{P(\boldsymbol{O}|\boldsymbol{I},\boldsymbol{\Theta})}{P(\boldsymbol{I})} \\ \geqslant& P(\boldsymbol{O}|\boldsymbol{\Theta})\sum_{\boldsymbol{I}} P(\boldsymbol{I})\log\frac{P(\boldsymbol{O}|\boldsymbol{I},\boldsymbol{\Theta})}{P(\boldsymbol{I})} \\ =& P(\boldsymbol{O}|\boldsymbol{\Theta})\sum_{\boldsymbol{I}} P(\boldsymbol{I})\log P(\boldsymbol{O},\boldsymbol{I}|\boldsymbol{\Theta}) \\ =& \sum_{\boldsymbol{I}} P(\boldsymbol{O},\boldsymbol{I}|\boldsymbol{\Theta})\log P(\boldsymbol{O},\boldsymbol{I}|\boldsymbol{\Theta}) \\ \geqslant& Q(\boldsymbol{\Theta},\hat{\boldsymbol{\Theta}}). \end{aligned} \tag{15}$$

The first inequality sign is due to the convex property of the log function, and the second inequality sign is due to the definition of function Q.

According to the definition of a Markov chain,

$$\begin{aligned} P(\boldsymbol{O},\boldsymbol{I}|\hat{\boldsymbol{\Theta}}) =& \pi_{i_1}\mathcal{N}_{i_1}(o_1)a_{i_1 i_2}\cdots \\ &\times \mathcal{N}_{i_{L-1}}(o_{L-1})a_{i_{L-1}i_L}\mathcal{N}_{i_L}(o_L). \end{aligned} \tag{16}$$

Thus, the function Q can be expressed as

$$\begin{aligned} Q(\boldsymbol{\Theta},\hat{\boldsymbol{\Theta}}) =& \sum_{\boldsymbol{I}} \log\pi_{i_1} P(\boldsymbol{O},\boldsymbol{I}|\hat{\boldsymbol{\Theta}}) \\ &+ \sum_{\boldsymbol{I}}\left(\sum_{l=1}^{L-1}\log a_{i_l i_{l+1}}\right)P(\boldsymbol{O},\boldsymbol{I}|\hat{\boldsymbol{\Theta}}) \\ &+ \sum_{\boldsymbol{I}}\left(\sum_{l=1}^{L}\log\mathcal{N}_{i_l}\right)P(\boldsymbol{O},\boldsymbol{I}|\hat{\boldsymbol{\Theta}}). \end{aligned} \tag{17}$$

Then, the optimal $\boldsymbol{\Theta}$ can be calculated by optimizing $\boldsymbol{A}$, $\boldsymbol{B}$, and $\boldsymbol{\pi}$ separately. The iteration method is used to find parameter $\boldsymbol{\Theta}$ to let Q reach its upper bound:

$$\boldsymbol{\Theta}^{(i)} = \arg\max_{\boldsymbol{\Theta}} Q(\boldsymbol{\Theta},\boldsymbol{\Theta}^{(i-1)}). \tag{18}$$

It was proven in Ref. [19] that by using the iteration of Eq. (14), the value of Q could reach one of the local optimums of function F. The initial value of $\hat{\boldsymbol{\Theta}}$ needs to be changed several times to the global optimum. The final $\boldsymbol{\Theta} = (\boldsymbol{A},\boldsymbol{B},\boldsymbol{\pi})$ is expressed as

$$\begin{aligned} \boldsymbol{A} =& \begin{bmatrix} 0.3049 & 0.6951 \\ 0.1041 & 0.8959 \end{bmatrix}, \\ \boldsymbol{B} =& \begin{bmatrix} \mathcal{N}(\theta_{10}|22.8744,1.6569) \\ \mathcal{N}(\theta_{10}|21.2363,1.1565) \end{bmatrix}, \\ \boldsymbol{\pi} =& [0,1]. \end{aligned} \tag{19}$$

The log-likelihood function is introduced to describe the probabilities of the experimental results under the normal distribution and the distribution of the Markov chain. The function is monotonically increasing with the likelihood of experimental data under a certain model. Thus, the log-likelihood function can represent the degree of confidence to some extent.

$$\begin{aligned} F[\theta_{10}|\mathcal{N}(\mu(\theta_{10}),\sigma^2(\theta_{10}))] &= -3.2258\times 10^{-3}, \\ F[\theta_{10}|\boldsymbol{\Theta} = (\boldsymbol{A},\boldsymbol{B},\boldsymbol{\pi})] &= -3.2022\times 10^{-3}. \end{aligned} \tag{20}$$

A normal distribution defined by the experimental mean $\mu(\theta_{10})$ and variance $\sigma^2(\theta_{10})$ is introduced in contrast. The log-likelihood is that a Markov chain defined by $\boldsymbol{\Theta}$ is slightly larger than that of the contrastive normal distribution. Thus, the Markov chain is more likely to generate the experimental results, and it is reasonable to determine parameter θ_{10} by the fitted Markov chain according to the experiment results.

Still, a simple explanation of the Markov chain is needed. The θ_{10} generated by the Markov chain is a description of the ignition delay of in-cylinder combustion. According to the Markov chain $\boldsymbol{\Theta}$, the ignition is divided into the following two categories: abnormal ignition and normal ignition. Abnormal ignition corresponds to the first state of $\boldsymbol{B}$, and normal ignition corresponds to the second. The ignition delay of abnormal ignition is unstable and longer on average than that of normal ignition as defined by $\boldsymbol{B}$. Moreover, as an explanation of matrix $\boldsymbol{A}$, normal ignition is more likely to occur regardless of whether the last ignition is normal or abnormal. However, an abnormal ignition is more likely to lead to another abnormal one than normal ignition. The above explanation is practical because abnormal ignition may lead to unstable combustion. The temperature and fraction of residual gas may vary greatly due to the unstable combustion of the last cycle. Then, abnormal ignition is more likely to occur.

B. Combustion model

When modeling the cyclic varied in-cylinder combustion, a functional description ranging from determinism to randomness is needed [13]. The Wiebe function, a frequently used equation, is chosen to simulate combustion [17]:

$$x_b = 1 - e^{-a(\frac{\theta}{\theta_{90}})^{m+1}}, \tag{21}$$

$$m = \frac{\ln 0.9}{\ln(\theta_{10}/\theta_{90})},\ a = \ln 0.1, \tag{22}$$

where θ is the crank angle, a and m are the nondimensional parameters calculated according to the definition of θ_{90} and θ_{10}, respectively, and x_b is the fraction of fuel burned at the crank angle θ.

The fraction of fuel burned can be regarded as a symbol of the combustion process. θ_{90} and θ_{10} are given in the first parts of the current model. Then, the heat release at each crank angle θ is calculated as follows:

$$\frac{dQ}{d\theta} = Q_{\text{total}} \frac{dx_b}{d\theta}, \tag{23}$$

where Q_{total} is the total heat release of the current cycle that is received from the first part of the current model.

Ignoring the thermal losses, the change in in-cylinder pressure p is given as

$$\frac{dp}{d\theta} = \frac{\kappa - 1}{V}\left(\frac{dQ}{d\theta} - \frac{\kappa}{\kappa - 1} p \frac{dV}{d\theta}\right), \tag{24}$$

where V is the cylinder volume at the present crank angle, and κ is the heat capacity ratio of the gas-oil mixture. In this paper, $\kappa = 1.32$ and the fluctuation of κ are ignored. Meanwhile, the initial value p_{IVC} of in-cylinder pressure p is the pressure when the intake value closes. p_{IVC} equals the intake manifold pressure of the engine nominal condition.

C. Knock model

In this part of the model, an existing method is used to detect knock based on the in-cylinder pressure. According to this method, the relationship between the knock probability and the parameter distribution is derived. Bayesian estimation is also applied to calculate the knock probability.

1. Integral predictable model

The Livengood-Wu integral predictable knock model, which is based on the Arrhenius function, is used to detect knock. This model divides the cylinder into burned and unburned zones. Each zone is considered homogeneous in terms of temperature, pressure, and gas mixture composition. Knock occurs when spontaneous ignition happens in the unburned zones [20]. Under certain environmental conditions, the self-ignition delay τ can be expressed as

$$\tau = C_1 \left(\frac{O_N}{100}\right)^{C_2} p^{-C_3} e^{\frac{C_4}{T_{\text{ub}}}}, \tag{25}$$

where C_1, C_2, C_3, and C_4 are the fitting coefficients. Thus, under a varying environment, the self-ignition index is defined as an integral of $1/\tau$, and self-ignition occurs when the index $I = 1$. At this point, knock happens,

$$I = \int_{t_{\text{IVC}}}^{t} \left(\frac{1}{\tau}\right) dt, \tag{26}$$

where T_{ub} is the unburned gas temperature that can be calculated based on an adiabatic assumption.

$$T_{\text{ub}} = T_{\text{IVC}} \left(\frac{p}{p_{\text{IVC}}}\right)^{1-\frac{1}{\kappa}} \tag{27}$$

T_{IVC} and p_{IVC} are the temperature and pressure when the intake value closes, $p_{\text{IVC}} = 0.6$ bar according to the experiment, and T_{IVC} equals the environment temperature.

The values of parameters C_2, C_3, and C_4 are given in the scientific literature [21]:

$$C_2 = 3.402, \quad C_3 = 1.700, \quad C_4 = 3800. \tag{28}$$

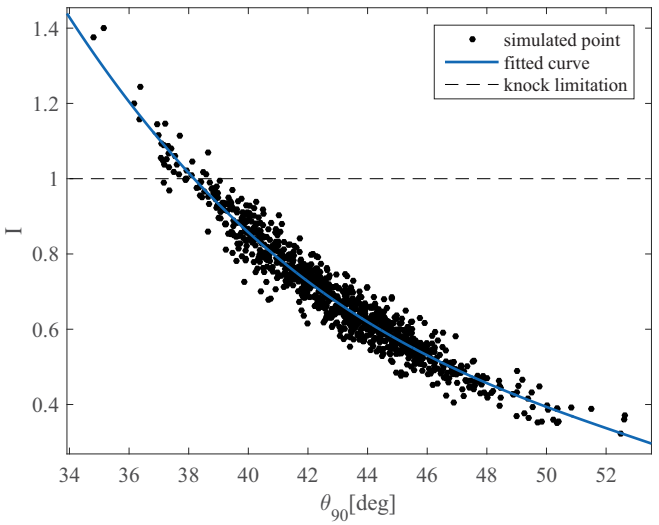

FIG. 10. Fitted relationship between the Livengood-Wu knock integration I and θ_{90}.

Parameter C_1 is modified to make the knock rate consistent with the experimental results:

$$C_1 = 12.91. \tag{29}$$

2. Parameter adjusting based on the knock model

In the same nominal operating conditions, the knocking probability changes by the immeasurable disturbance of environment. To characterize this phenomenon, a simulator generating a series of combustion of given knocking probability is needed. It is reasonable to assume that the mean value of the model parameters are decided by the nominal operating conditions. The knock probability fluctuation due to the immeasurable disturbance is reflected by the alteration of the variance of model parameters. The σ_θ^2, variance of θ_{90} is selected to describe the environment fluctuation. Moreover, the σ_Q^2 variance of Q_{total} calculated by σ_θ^2 varies along with environment.

It is clear that if the knock probability equals 3%, which is same as the experiment result, the variance of θ_{90} is 4.6115 and equals the experimental value. The variance of θ_{90} under other knock probabilities needs to be calculated. One thousand cycles under the 3% knock probability are simulated, and the Livengood-Wu integration I is calculated. The lower θ_{90}, which indicates quicker combustion, is likely to generate higher Livengood-Wu integration, leading to high knock probability, as illustrated in Fig. 10.

θ_{90} and I are fitted by a cubic polynomial as follows:

$$I = f(\theta_{90}) = -8.551e - 5 \times \theta_{90}^3 + 0.01366 \times \theta_{90}^2 - 0.7537 \times \theta_{90} + 14.63. \tag{30}$$

The estimated limitation of knock $\theta_{90}^\star = 38.18$ can be obtained by the solution of $f(\theta_{90}^\star) = 1$. According to the fitted curve of θ_{90} and I, if θ_{90} is less than $\theta_{90}^\star$ in this nominal operating condition, the Livengood-Wu integration I is likely more than 1, and then knock happens. Thus, the distribution of θ_{90} can determine the knock probability to a certain degree; although, the randomness of Q_{total} and θ_{10} can also affect the knock

probability. Therefore, when the knock probability K is given,

$$P(\theta_{90}|\theta_{90} < 38.1) \simeq P(I|I > 1) = K. \tag{31}$$

The variance of θ_{90} is chosen to be σ_θ^{2*} to adjust the knock probability into the given value:

$$\sigma_\theta^{2*} = \frac{\mu_\theta - \theta_{90}^\star}{\mathcal{N}^{-1}(1-K)}, \tag{32}$$

where $\mathcal{N}^{-1}$ means the inverse function of the cumulative density function of the standard normal distribution. By replacing the original variance $\sigma_\theta^2 = 4.6115$ with the newly calculated σ_θ^{2*}, the combustion and knock can be simulated.

3. Bayesian estimation of knock probability

To explain the accuracy of the proposed simulator, a precise estimation of knock probability is needed. A Bayesian estimation is selected to calculate the knock probability K^*. Furthermore, whether knock occurs is a binomial distribution. For the sake of convenience, a β distribution with coefficients α and β is selected to describe the knock probability as a prior distribution because the β distribution is a conjugate prior distribution of binomial distribution, and the calculation can be simplified using conjugate prior distribution:

$$p(K^*) = \mathcal{B}(\alpha,\beta). \tag{33}$$

Under this assumption, the expectation of the knock probability is used as the estimation of knock probability and can be calculated as

$$E(K^*) = \frac{\alpha}{\alpha+\beta}. \tag{34}$$

The β distribution of knock probability is updated on the basis of the simulated results of whether knock occurs. According to the Bayesian estimation, α and β are updated in the ith cycle:

$$\begin{aligned} \alpha_i &= \alpha_{i-1} + k_i, \\ \beta_i &= \beta_{i-1} + 1 - k_i, \end{aligned} \tag{35}$$

where k_i is a dummy symbol of knock. $k_i = 1$ means knock happens. The initial value of α and β is given on the basis of the given knock probability K:

$$\begin{aligned} \alpha_0 &= NK, \\ \beta_0 &= N(K-1). \end{aligned} \tag{36}$$

D. Simulated results

According to the combustion model and the generated random parameters, the in-cylinder pressure during continuous 1000 cycles indicates that the operating conditions of the simulation are same as the experimental conditions.

As mentioned above, knock is an abnormal phenomenon of in-cylinder combustion. Thus, it is reasonable to set a low given knock probability. The given probability are set to 1%, 3%, and 5%. The proposed simulator successfully provides the in-cylinder pressure with cycle-to-cycle variation. The simulated in-cylinder pressure of 1000 consecutive cycles is presented in Fig. 11. The oscillation range of maximum pressure ($\triangle P_m$) can illustrate the cycle-to-cycle variation. Figure 11(a) shows the in-cylinder pressure curves when a given knock probability equals 1%, and the oscillation range of maximum pressure $\triangle P_{m1} = 15.85$ bar; Fig. 11(b) shows when

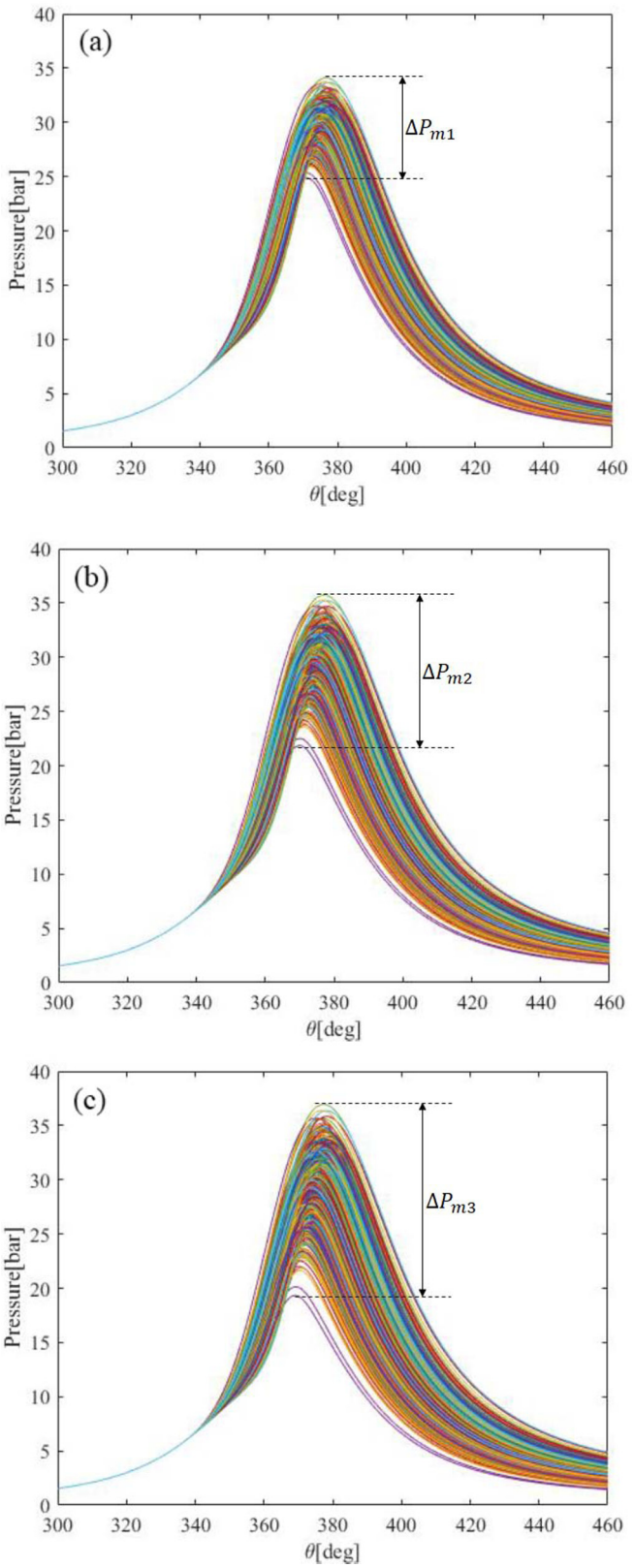

FIG. 11. Simulated in-cylinder pressure for 1000 cycles. (a) Given knock probability $K = 0.01$. (b) Given knock probability $K = 0.03$. (c) Given knock probability $K = 0.05$.

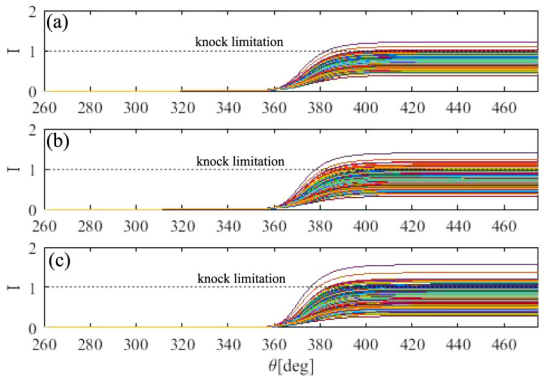

FIG. 12. Simulated Livengood-Wu knock integration I for 1000 cycles. (a) Given knock probability $K = 0.01$. (b) Given knock probability $K = 0.03$. (c) Given knock probability $K = 0.05$.

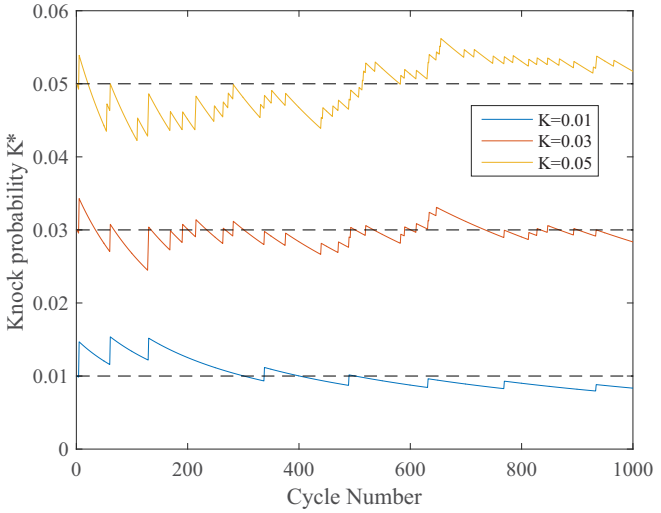

FIG. 13. Simulated Livengood-Wu knock integration I for 500 cycles.

the probability equals 3%, $\triangle P_{m2} = 19.96$ bar; and Fig. 11(c) shows 5%, $\triangle P_{m2} = 20.13$ bar.

Combustion begins when the crank angle reaches 344 degrees since the in-cylinder curves diverge from one cycle to another, which is the same as the experimental results. Figure 11 shows in this simulation that when the given knock probability becomes higher, combustion is more unstable, and the curves of the simulated in-cylinder pressure become more dispersive. This matches the results of the real experiment.

According to the simulated pressure, the Livengood-Wu integration I is calculated as shown in Fig. 12. In Fig. 12, knock happens when the solid lines that represent the Livengood-Wu knock integration I exceed the knock limitation marked by the dashed lines. When the given knock probability becomes higher, more curves of calculated Livengood-Wu knock integration I exceed the dashed line.

As shown in Fig. 13, the solid line shows the simulated knock probabilities calculated by the Bayesian estimation, and the dashed lines represent the given knock probabilities. The simulated knock probability is increased when knock happens in this cycle, otherwise it is decreased. The changing range of knock probability during one cycle reduces, because the simulated data applied in Bayesian estimation is accumulated. The simulated knock probabilities are 0.8%, 2.8%, and 5.2% after the calculation of 1000 cycles, which are close to the given points.

By analyzing the simulation result, it can be inferred that this simulator can describe the engine combustion based on the physical background and simulate the cycle-to-cycle variation according to real experiment properties. Moreover, the proposed model can simulate the in-cylinder combustion under different knock probabilities.

V. CONCLUSION

In this paper, an approach is developed to simulate the stochastic and deterministic characteristics of in-cylinder combustion, which are further applied to simulate given knock probabilities by a 1D dynamic model. A multivariate normal distribution and a Markov chain were introduced to describe the randomness of combustion. A dynamic equation and the Wiebe function are selected to explain the determinants of combustion. The Livengood-Wu integration is used to estimate whether knock happens.

In the proposed model, the combustion and in-cylinder pressure are determined by the combustion parameters. The mean values of the combustion parameters are determined by the nominal operating conditions according to the experimental data, and the variance of several combustion parameters are affected by the given knock probability.

This 1D dynamic model is simple enough, so the calculation can well match actual engine operation. Therefore, this model can be used in the real-time control of spark-ignition engines. It should be noted that in this paper, a static operation engine model is targeted to simulate the knock probability. Hence, the parameter depends on the operating conditions. If the conditions change, then the parameters should be recalibrated.

ACKNOWLEDGMENTS

This work is supported by Council for Science, Technology and Innovation (CSTI), Cross-ministerial Strategic Innovation Promotion Program (SIP), Innovative Combustion Technology (Funding agency: JST). We thank Prof. Y. Moriyushi and Prof. T. Kuboyama for providing insight and a deep discussion that greatly assisted this research.

[1] N. T. Bharath, S. A. Rashkovskiy, S. P. Tewari, and M. K. Gundawar, Phys. Rev. E **87**, 042804 (2013).

[2] H. Gotoda, Y. Shinoda, M. Kobayashi, Y. Okuno, and S. Tachibana, Phys. Rev. E **89**, 022910 (2014).

[3] H. Gotoda, Y. Okuno, K. Hayashi, and S. Tachibana, Phys. Rev. E **92**, 052906 (2015).
[4] N. Ozdor, M. Dulger, and E. Sher, Cyclic variability in spark ignition engines a literature survey, SAE Technical Paper 940987 (SAE International, Warrendale, PA, 1994).
[5] K. S. Kim and J. Ghandhi, A simple model of cyclic variation, SAE Technical Paper 2012-32-0003 (SAE International, Warrendale, PA, 2012).
[6] E. Hellström, A. G. Stefanopoulou, and L. Jiang, IEEE Trans. Control Syst. Technol. **21**, 1527 (2013).
[7] C. E. Finney, B. C. Kaul, C. S. Daw, R. M. Wagner, K. D. Edwards, and J. B. Green, Jr., Int. J. Engine Res. **16**, 366 (2015).
[8] T. Lee, R. Prucka, and Z. Filipi, Proc. Inst. Mech. Eng., Part D **223**, 1361 (2009).
[9] M. Wenig, M. Grill, and M. Bargende, SAE Int. J. Engines **6**, 1099 (2013).
[10] C. Poetsch, H. Schuemie, H. Ofner, R. Tatschl, and O. Vitek, A computational study on the impact of cycle-to-cycle combustion fluctuations on fuel consumption and knock in steady-state and drivecycle operation, SAE Technical Paper 2013-24-0030 (SAE International, Warrendale, PA, 2013).
[11] C. S. Daw, M. B. Kennel, C. E. A. Finney, and F. T. Connolly, Phys. Rev. E **57**, 2811 (1998).
[12] A. Karvountzis-Kontakiotis, L. Ntziachristos, Z. Samaras, A. Dimaratos, and M. Peckham, Experimental investigation of cyclic variability on combustion and emissions of a high-speed SI engine, SAE Technical Paper 2015-01-0742 (SAE International, Warrendale, PA, 2015).
[13] F. Millo, L. Rolando, E. Pautasso, and E. Servetto, A methodology to mimic cycle to cycle variations and to predict knock occurrence through numerical simulation, SAE Technical Paper 2014-01-1070 (SAE International, Warrendale, PA, 2014).
[14] Y. Zhang, J. Gao, and T. Shen, IEEE Trans. Neural Netw. Learn. Syst. 1 (2017).
[15] D. Upadhyay, *Modeling and Model Base Control Design of the VGT-EGR System for Intake Flow Regulation in Diesel Engines*, Ph.D. thesis, Ohio State University, 2001.
[16] R. Isermann, *Engine Modeling and Control* (Springer, Berlin/Heidelberg, 2014).
[17] L. Eriksson and L. Nielsen, *Modeling and Control of Engines and Drivelines* (John Wiley & Sons, New York, 2014).
[18] C. M. Bishop, *Pattern Recognition and Machine Learning* (Springer Science and Business, Berlin, 2006).
[19] S. K. Ng, T. Krishnan, and G. J. McLachlan, in *Handbook of Computational Statistics* (Springer, Berlin, 2012), pp. 139–172.
[20] Y. Chen and R. Raine, Combust. Flame **162**, 2108 (2015).
[21] L. Chen, T. Li, T. Yin, and B. Zheng, Energy Convers. Manage. **87**, 946 (2014).